# Autonomous Control of Current- and Voltage-Controlled DG Interface Inverters for Reactive Power Sharing and Harmonics Compensation in Islanded Microgrids

Mousazadeh, Seyyed Yousef ; Jalilain, Alireza; Savaghebi, Mehdi; Guerrero, Josep M.

*Published in:*
I E E E Transactions on Power Electronics

*DOI (link to publication from Publisher):*
10.1109/TPEL.2018.2792780

*Publication date:*
2018

*Document Version*
Accepted author manuscript, peer reviewed version

This article has been accepted for publication in a future issue of this journal, but has not been fully edited. Content may change prior to final publication. Citation information: DOI 10.1109/TPEL.2018.2792780, IEEE Transactions on Power Electronics



# Autonomous Control of Current and Voltage Controlled DG Interface Inverters for Reactive Power Sharing and Harmonics Compensation in Islanded Microgrids

Seyyed Yousef Mousazadeh Mousavi, Alireza Jalilian, Mehdi Savaghebi, *Senior Member, IEEE* and Josep M. Guerrero, *Fellow, IEEE*

***Abstract*— In microgrids, Voltage Source Inverters (VSIs) interfacing Distributed Generation (DG) units can be operated in Voltage or Current Controlled Modes (VCM/CCM). In this paper, a coordinated control of CCM and VCM units for reactive power sharing and voltage harmonics compensation is proposed. This decentralized control scheme is based on the local measurement of signals. In this way, the need for communication links is removed which results in a simpler and more reliable structure compared to the communication based control structures. To be more exact, the VCM units contribute to harmonics compensation by using capacitive virtual impedance which can fully compensate the effect of output inductance of the LCL filters. Furthermore, an adaptive virtual admittance regulated based on remaining capacity of the CCM units is implemented for the CCM units. For reactive power sharing, modified droop and reverse droop control methods are used for VCM and CCM units, respectively. The related droop coefficients are set by taking the limited capacity of the inverters and the distorted power into account. An experimental prototype is developed to evaluate the effectiveness of the proposed control scheme. Experimental and simulation studies show that the harmonics compensation is achieved by using only local measurements in presence of virtual admittance/impedance schemes of CCM/VCM units. Furthermore, it is demonstrated that the reactive power sharing among the CCM and VCM units is obtained based on their remaining capacities.**

***Index Terms*— current controlled mode, Distributed Generation (DG), harmonic compensation, microgrid, reactive power, voltage controlled mode, voltage source inverter.**

## I. Introduction

VOLTAGE Source Inverters (VSIs) are widely used as interfaces of Distributed Generation (DG) units in distribution systems and microgrids (MGs) [1], [2]. They can be operated in Current/Voltage Control Modes (CCM/VCM) depending on the operation modes of MGs and the nature of DG resources [3]. In MGs, the energy storage systems and controllable (dispatchable) DGs often act as voltage-controlled inverters while the intermittent Renewable Energy Sources (RESs) based (non-dispatchable) DGs such as Photovoltaic (PV) systems and Wind Turbines (WT) are interfaced to the system through CCM inverters [4]. Usually, CCM units are supposed to inject maximum available active power while VCM units deliver active and reactive powers and control voltage and frequency especially in the islanded operation of MGs [5].

For VCM units, decentralized, centralized and distributed control schemes are presented for active and reactive power sharing [6]-[8]. In [9] and [10], the reactive power compensation in distribution systems by DG CCM units is discussed. In [11] and [12], the coordinated control of active and reactive powers of VCM and CCM inverters is proposed. The methods of [11] and [12] are based on droop and reverse droop controls, which use local measurement. By using these control schemes, the CCM inverters can contribute to reactive power sharing in an islanded MG. Although, the limited capacity of the inverters is considered in [11], this approach is not comprehensive enough since only linear loads are taken into account.

On the other hand, the increasing use of nonlinear loads has led to the harmonic pollution in electrical systems [13]. Control of DGs interfacing inverters for compensation of harmonics in MGs and DG-penetrated systems are investigated [14]-[24].

The use of secondary control for the compensation of harmonics by VCM units is proposed in [15] and [16]. In these hierarchical architectures, some communication links and a central control are required, which increases the cost and decreases the system reliability. The harmonic compensation using capacitive-resistive virtual impedance is presented in [17]-[19] for VCM units. In these methods, the distorting effect of harmonic voltage drops on the line and filter impedances is compensated for enhancing the power quality using local measurements. The compensation of voltage and current is also presented in [20] where the VCM inverters can compensate the local nonlinear load current, DG or PCC voltages selectively. The methods presented in [15]-[20] are

S. Y. Mousazadeh and A. Jalilian are with Department of Electrical Engineering Iran University of Science and Technology, Tehran-Iran. A. Jalilian is also with Center of Excellence for Power System Automation and Operation, Iran University of Science and Technology (e-mail: s_y_mosazade@iust.ac.ir; jalilian@iust.ac.ir)

M. Savaghebi and J. M. Guerrero are with the Department of Energy Technology, Aalborg University, Aalborg, Denmark (e-mail: mes@et.aau.dk; joz@et.aau.dk)

This article has been accepted for publication in a future issue of this journal, but has not been fully edited. Content may change prior to final publication. Citation information: DOI 10.1109/TPEL.2018.2792780, IEEE Transactions on Power Electronics



proposed for VCM units while CCM units are typically applied and may contribute to harmonics compensation in MGs.

Moreover, grid-connected CCM inverters are employed in [21]-[23] for local harmonic current compensation and PCC voltage quality enhancement. In [21], a coordinated control for the compensation of grid voltage harmonics and local nonlinear load current is proposed for two CCM units. Limited capacity of the inverters is considered in compensation of harmonics and reactive power of grid connected MG in [22]. However, in this scheme, the measurement of injected current and a central controller is required which can increase the complexity of the system. The harmonics compensation by grid tied inverters considering the limited virtual admittance of the inverter is presented in [23]. In the method of [23], the control of active and reactive powers is achieved by using fundamental-frequency virtual admittance while for the harmonics compensation; a virtual admittance with a fixed value in harmonic frequencies is applied. It should be emphasized that the method of [21] - [23] are applied only to grid-tied CCM inverters.

A coordinated control method for CCM and VCM units by using a central controller (based on the communication system) and virtual admittance is proposed in [24]. However, in this study, the limited capacity and reactive power sharing of the CCM and VCM units are not considered.

In the present paper, the reactive power sharing method presented in [11] is improved by considering the distorted power (i.e., the power drawn by nonlinear loads) according to IEEE 1459 standard [25]. Unlike the method proposed in [24], the harmonic compensation by CCM and VCM units is autonomously coordinated based on the local measurements. In this way, the need for the communication is removed leading to a more reliable and simpler control strategy as compared with communication-based approaches. The virtual capacitive impedance is used in VCM units for compensation of harmonic voltage drop on the output inductance of the LCL filter. In this study, the virtual admittance is dynamically set based on the remaining capacity of the inverters to share CCM unit's harmonic compensation efforts. This approach is desired in application of CCM units where the reference power varies frequently in different operating conditions.

The main contributions of the paper can be summarized as follows:

- Proposing a communication-free control method for the coordinated harmonic compensation and reactive power support by CCM and VCM units based on local measurements
- Considering the distorted power and the remaining capacity of the interface inverters for reactive power compensation of VCM and CCM units
- Taking into account the changes in the reference power of CCM units for harmonics and reactive power compensation

The remaining parts of the paper are presented as follows: In Section II, the general control scheme and reactive power control method are presented. Section III is dedicated to present the VCM and CCM control schemes. Simulation and experimental results are presented in Section IV and finally, the paper is concluded in Section V.

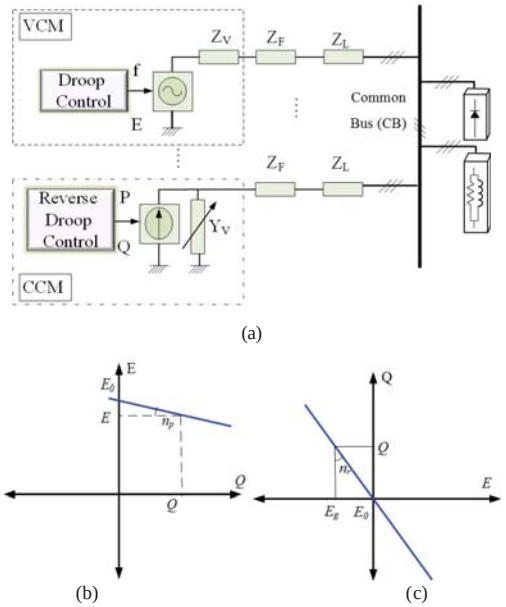


Fig. 1. Coordination of CCM and VCM units in an MG, (a) general scheme of an islanded MG including CCM, VCM units, (b) reactive power droop control, (c) reverse reactive power droop control [11]

## II. General Control Scheme of the MG

General scheme for an MG including current and voltage controlled inverters is depicted in Fig. 1(a). In this figure, $Z_V$, $Z_F$ and $Z_L$ represent the virtual, filter and line impedances, respectively and $Y_V$ is the virtual admittance. Linear and nonlinear loads are connected to the load connection point, hereinafter called Common Bus (CB). Typically, VCM units control and regulate the frequency and voltage amplitude of the MG while the maximum power values extracted from DG units such as PV and WT are injected to the MG by CCM inverters [26], [27].

Droop control is widely used in VCM inverters for the autonomous sharing of active and reactive powers. Assuming a highly inductive MG, the droop control is expressed by (1) [28]:

$$\omega = \omega_0 - m_p P,\ E = E_0 - n_p Q \qquad (1)$$

where $\omega_0$ and $\omega$ denote the rated and actual voltage angular frequencies. Rated and actual voltage amplitude values are represented by $E_0$ and $E$, respectively. $m_p$ and $n_p$ are the proportional coefficients related to active and reactive powers droops of VCM units, respectively. It is worth mentioning that even if the MG under study is not highly inductive, the fundamental virtual inductance may help to make it inductive enough [6]. The graphical representation of reactive power droop control for VCM units is shown in Fig. 1(b).

The contribution of CCM inverters in the active and reactive powers sharing is achieved by using the reverse droop control as:

$$Q = \frac{1}{n_r}(E_0 - E_g)\ \ P = \frac{1}{m_r}(\omega_0 - \omega_g), \qquad (2)$$

This article has been accepted for publication in a future issue of this journal, but has not been fully edited. Content may change prior to final publication. Citation information: DOI 10.1109/TPEL.2018.2792780, IEEE Transactions on Power Electronics



where $\omega_g$ and $E_g$ represent the system actual angular frequency and RMS voltage at the point of connection of CCM inverters, respectively [11]. The output active and reactive powers of the CCM unit are represented by $P$ and $Q$ while mr and nr are the reverse droop coefficients for CCM units. As mentioned before, CCM units usually deliver the reference power which is extracted by Maximum Power Point Tracking (MPPT) systems (in the case of PV and WT), power curtailment strategies [26], energy management strategies [29], [30] or emergency control [5], [26], [31]. Hence, in this paper, it is assumed that $P=P_{max}$ which means that active reverse droop of (2) does not act for CCM units and the remaining load active power is supplied by the VCM units. In other words, the details of generating active power references for the CCM units are out of the scope of the present paper. The reactive power sharing of CCM units by reverse droop has been shown in Fig. 1(c).

By neglecting the voltage drops, the sharing of reactive power among the DGs (including VCM and CCM units) can be written as:

$$\frac{Q_i}{Q_j}=\frac{n_j}{n_i} \tag{3}$$

where $n_i$ and $n_j$ represent the droop/ reverse droop reactive power coefficients ($n_p/n_r$) of i$^{th}$ and j$^{th}$ VCM/CCM units [11].

In a distorted grid, the harmonic current and voltage can occupy the capacity of the inverters. According to IEEE 1459 standard, the apparent power ($S$) consists of three components ($S_N$, $P$ and $Q$) as described as follows [25]:

$$S^2=S_N^2+P^2+Q^2=S_N^2+S_1^2 \tag{4}$$

$$S_N^2=(V_1I_H)^2+(V_HI_1)^2+(V_HI_H)^2 \tag{5}$$

where $S_1$ and $S_N$ represent the fundamental apparent and distorted harmonics powers, respectively. $V_1$ and $I_1$ are the RMS fundamental voltage and current while $V_H$ and $I_H$ represent the RMS of harmonics contents of voltage and current. Without significantly affecting the accuracy, $S_N$ can be well approximated by $S_N\approx V_1I_H$ since $V_1I_H$ is the dominant term in (5) [25].

In this paper, the power quality enhancement by the CCM inverters is prioritized over the reactive power compensation since an islanded MG is more prone to harmonics distortion in comparison to a grid-connected one [15]. In other words, when the rated capacity of the inverter is defined as $S_r$, first and foremost the remaining capacity of the inverter (i.e. $\sqrt{S_r^2-P^2}$) is allocated to the harmonic compensation. After computing the distorted power ($S_N$), the rest of capacity is allocated to reactive power compensation. Indeed, the priority can be given to reactive power compensation by changing the order of calculations if it is more important for the system operator using $K_{prio}$ parameter. If the power quality enhancement is prioritized over reactive power compensation, the amount of this parameter should be 1. If else, the reactive power compensation is prioritized by setting this parameter to zero. In this paper, the amount of $K_{prio}$ is considered equal to 1. Hence, according to the above equation, the maximum injectable reactive power of CCM and VCM units can be expressed as:

$$Q_{\max}=\sqrt{S_r^2-P^2-K_{prio}\cdot S_N^2} \tag{6}$$

This equation shows that the available reactive power support, in addition to the rated capacity of the inverter and $P$, depends on $S_N$ and $K_{prio}$.

In order to use the remaining capacity of the inverters, the reactive power droop and reverse droop control coefficients, which are expressed in (1) and (2) respectively, are suggested here to be calculated based on the available capacity for reactive power support:

$$n_r=n_p=n=\frac{\Delta E}{Q_{\max}}=\frac{\Delta E}{\sqrt{S_r^2-P^2-K_{prio}\cdot S_N^2}} \tag{7}$$

where $\Delta E$ represents the maximum allowable voltage amplitude deviation. By replacing this equation in (2), the injectable reactive power of CCM units can be written by (8):

$$Q=\frac{1}{n_r}(E_0-E_g)=\frac{1}{n}(E_0-E_g)=\frac{\sqrt{S_r^2-P^2-K_{prio}\cdot S_N^2}}{\Delta E}(E_0-E_g) \tag{8}$$

As depicted in (8) and Fig. 1(c), the CCM unit can react to the voltage amplitude deviation ($E_0$-$E_g$). If the voltage deviation is high, the DG contributes more to reactive power compensation. As expressed in (8), the rate of the reaction is dependent on $1/n$. If the remaining capacity of the inverter reaches zero, according to (8), the slope of reverse droop shown in Fig. 1(c) will be zero and the DG cannot contribute to reactive power compensation. If the active power of DG is low and the DG does not contribute to harmonics compensation, the available reactive power compensation of DG will be increased to its maximum and the corresponding $n$ will be decreased to its minimum. It causes increase reverse droop slope (see Fig. 1(c)); hence the reactive power contribution will be increased.

It should be mentioned that since n is directly applied for droop control of VCM units according to (1), a saturation block is used for the denominator of (7) to avoid division by zero.

According to (7), Eq. (3) can be rewritten as (9):

$$\frac{Q_i}{Q_j}=\frac{\sqrt{S_{r,i}^2-P_i^2-K_{prio}\cdot S_{N,i}^2}}{\sqrt{S_{r,j}^2-P_j^2-K_{prio}\cdot S_{N,j}^2}} \tag{9}$$

This reactive power sharing is useful in islanded microgrid, because when the active power of CCM units is high and the active power delivered by VCM units is low, the VCM units can deliver more reactive power than CCM units while if the CCM delivered power is low and VCM units deliver high power, the CCM units can inject more reactive power to MG; Furthermore, If harmonics compensation is prioritized over than reactive power compensation ($K_{prio}$=1), the DG which

This article has been accepted for publication in a future issue of this journal, but has not been fully edited. Content may change prior to final publication. Citation information: DOI 10.1109/TPEL.2018.2792780, IEEE Transactions on Power Electronics



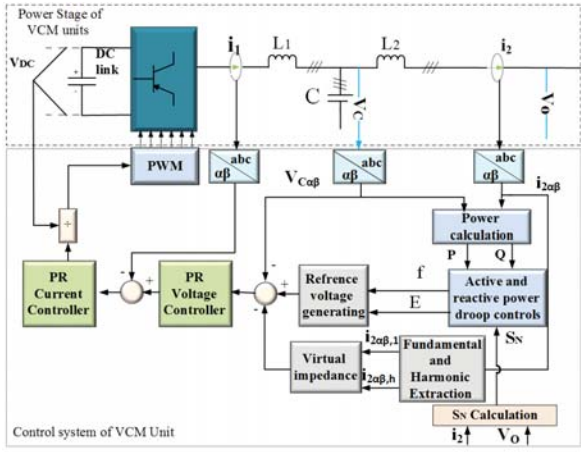


Fig. 2. The control and power stages of VCM and CCM units in a MG, (a) VCM unit; (b) CCM unit.

delivers more distorted power can contributes lower in reactive power sharing by considering equal rated apparent power ($S_r$) and active power. It shows the advantage of the modified droop and reverse droop control approach in comparison to the conventional ones.

## III. Control Scheme of VCM and CCM Units

The control and power stages of the VCM and CCM units are depicted in Figs. 2(a) and 2(b), respectively. As shown, the power stages of VCM and CCM units consist of a DC link, a three-phase inverter and an LCL filter. The control stages of these units are discussed in the following sections.

### A. VCM Unit

As depicted in Fig. 2(a), the three-phase current and voltage variables are converted to stationary frame variables (αβ) by using Clarke's transformation. Then, the fundamental active and reactive powers are calculated based on the instantaneous active and reactive power theory [32].The active and reactive powers droop controls are based on (1). The reactive power droop coefficient can be calculated by (7) while considering the distorted power ($S_N$).

The voltage and current control loops consist of Proportional-Resonant (PR) controllers with resonant terms at fundamental and selected harmonic frequencies (5th, 7th and 11th). More details about the droop and PR controllers can be found in [33]. The fundamental and harmonics extraction in Figs 2(a) and 2(b) are extracted by multiple second-order generalized integrator (MSOGI) method [34].

Since the *P-f* and *Q-V* droops are valid in inductive MGs, the inductive virtual impedance is utilized in the fundamental frequency (i.e. fundamental component currents $i_{2\alpha\beta,1}$ [subscript '1' represents the fundamental component] pass through a virtual inductance). Since the parameters of the lines are usually unknown, only the compensation of output inductance of LCL filter ($L_2$) is targeted by using the virtual impedance. In order to compensate the effect of filter output inductance $L_2$ on the voltage distortion, the capacitive virtual impedance is inserted selectively at low-order characteristic harmonics of order 5, 7, and 11 (i.e. $h^{th}$ harmonic current, $i_{2\alpha\beta,h}$ passes through a virtual capacitance depending on the sequence of the harmonics). More details about the capacitive virtual impedance can be found in [16].

### B. CCM Unit

As shown in Fig. 2(b), the interface inverter is connected through an LCL filter. Incorporation of LCL filters can inherently cause harmonic resonances; hence, an active resonance damping is applied through capacitor current feedback (see $K_D$ in Fig. 2(b)) and control of output current is performed through a multi-loop scheme [35]-[38]. In summary, the current inner loop is used for improving the dynamic and stability of the system while the tracking of the reference current is the role of the outer loop [37].

The resonant terms of PR controller are tuned at fundamental, 5th, 7th and 11th harmonic orders. Use of the PR controller can ensure accurate tracking of $i_2$ in fundamental and selected harmonic frequencies. In the control system, the capacitor or output voltage of LCL filter ($V_O$) can be measured and used as feedback [24]. Since the output voltage of the LCL filter ($V_O$) is closer to (CB) (see Fig. 2(b)), the control of this voltage (instead of the filter capacitor voltage) can be more effective for providing a good voltage quality at the CB. As can be seen in Fig. 2(b), the voltage amplitude ($E$) is compared to its reference value ($E_0$) and the reference reactive power is generated based on the proposed reverse control according to (2) and (7). The reference current for injecting the reference active and reactive powers are calculated based on the following equation:

$$\begin{bmatrix} I_{ref,\alpha} \\ I_{ref,\beta} \end{bmatrix} = \begin{bmatrix} V_{O1,\alpha} & V_{O1,\beta} \\ -V_{O1,\beta} & V_{O1,\alpha} \end{bmatrix}^{-1} \begin{bmatrix} P \\ Q \end{bmatrix} \quad (9)$$

The diagram of the virtual admittance block is depicted in Fig. 3(a). As it can be observed in this figure, after the harmonic extraction, the RMS amount of each harmonic ($V_{Oh}$) is divided by the fundamental component RMS ($V_{O1}$) in order to calculate $H_h$ which denotes the individual harmonic indices of $V_O$. As mentioned before, in this paper, a MSOGI is used for the extraction of the fundamental and harmonic components of the grid voltage and current [34]. The MSOGI accuracy and, therefore, the calculation of $H_h$ factors can be enhanced by increasing the number of parallel SOGIs, but at the cost of a high computational burden. To provide a satisfactory compromise, four parallel SOGIs tuned at fundamental, 5th,

This article has been accepted for publication in a future issue of this journal, but has not been fully edited. Content may change prior to final publication. Citation information: DOI 10.1109/TPEL.2018.2792780, IEEE Transactions on Power Electronics



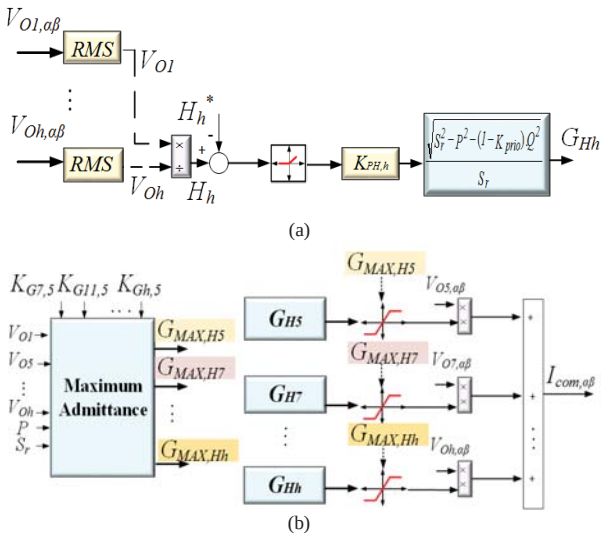


Fig. 3. Details of virtual admittance block of Fig 2(b); (a) $G_{Hh}$ calculation block; (b) overall scheme

7th and 11th harmonics frequencies have been selected in this paper.

Afterward, $H_h$ is compared to its allowable value, which is represented by $H_h^*$, and the resultant error passes through a deadband block in order to avoid the power quality compensation effort when it is not necessary. In other words, the inverter should not contribute to the harmonic compensation when $H_h$ is lower than $H_h^*$. The value of $H_h^*$ can be chosen based on a power quality standard (e.g. EN 50160 standard [39] and IEEE 519 standard [40]) or the sensitivity of the load to harmonics. Proportional controllers ($K_{PH,h}$) are used to regulate the amount of virtual admittance in each harmonic.

The sharing of harmonic compensation effort among CCM units is achieved by using the $\sqrt{S_r^2 - P^2 - (1-K_{prio})Q^2}/S_r$ gain. In order to avoid the overloading of the CCM units, the maximum value of the conductance $G_{Hh}$ ($G_{MAX,Hh}$) is calculated and applied to the dynamic limiter blocks according to Fig. 3(b). The maximum allowable value of $S_N$ is considered to be equal to the remaining capacity of the inverter and can be written according to the approximation explained after equation (5) as:

$$S_{N,\max} = \sqrt{S_r^2 - P^2 - (1-K_{prio}).Q^2} = V_{O1} \cdot I_{H,\max} \tag{11}$$

Thus, the maximum harmonic current ($I_{H,max}$) that can be injected by a CCM unit is expressed as:

$$I_{H,\max} = \frac{\sqrt{S_r^2 - P^2 - (1-K_{prio}).Q^2}}{Vo_1} = \frac{}{\sqrt{G^2_{MAX,H5}V^2_{O5} + G^2_{MAX,H7}V^2_{O7} + \ldots + G^2_{MAX,Hh}V^2_{Oh}}} \tag{12}$$

It should be mentioned that if $K_{prio}$ is set to 1 (harmonics compensation priority), the $\sqrt{S_r^2 - P^2}$ for harmonics compensation and if the variable is set to 0, the $\sqrt{S_r^2 - P^2 - Q^2}$ will be dedicated to harmonics compensation; furthermore, equation (12) with some unknown parameters can be used to calculate the maximum admittance of 5th harmonics by assuming $K_{Gh,5}$ as the ratio of the maximum admittance (conductance) of $G_{Hh}$ to $G_{H5}$ ($K_{Gh,5}$=$G_{MAX,Hh}$/$G_{MAX,H5}$):

$$S_{N,\max} = \sqrt{S_r^2 - P^2 - (1-K_{pri}).Q^2} = V_{O1} \cdot I_{H,\max} \tag{13}$$

Thus, the maxim harmonics current which can be injected by a CCM unit is expressed as:

$$G_{MAX,H5} = \frac{\sqrt{S_r^2 - P^2 - (1-K_{prio}).Q^2}}{V_{O1}\sqrt{V^2_{O5} + K^2_{G7,5}V^2_{O5} + K^2_{G11,5}V^2_{O11} + K^2_{Gh,5}V^2_{Oh}}} = \frac{\sqrt{S_r^2 - P^2 - (1-K_{prio}).Q^2}}{V^2_{O1}\sqrt{H^2_5 + K^2_{G7,5}H^2_7 + K^2_{G11,5}H^2_{11} + \ldots + K^2_{Gh,5}H^2_h}} \tag{14}$$

While the maximum admittance of 7th, 11th and $h^{th}$ order harmonics can be written as:

$$G_{MAX,H7} = K_{G7,5} \cdot G_{MAX,H5}, \ldots, G_{MAX,Hh} = K_{Gh,5} \cdot G_{MAX,Hh} \tag{14}$$

It should be mentioned that in this paper, for the sake of simplicity, it is assumed that the ratios ($K_{G7,5}$ and $K_{G11,5}$) are 1 (i.e. $G_{MAX,H5}$=$G_{MAX,H7}$= $G_{MAX,H11}$) although it can be chosen differently.

As shown in Fig. 4(b), the value of virtual admittances at each harmonics frequency is multiplied by its related voltage in $\alpha\beta$ frame ($V_{\alpha\beta,h}$) in order to create compensation currents at this frequency ($I_{com,h\alpha\beta}$). Finally, the compensation currents at different frequencies are added together to form the total compensation current ($I_{com,\ \alpha\beta}$).

## IV. Simulation and Experimental Results

In order to verify the effectiveness of the proposed method, some simulation and experimental results are presented. The rated apparent power of CCM inverters are assumed 10% higher than the maximum active power that can be extracted from the DG prime movers (e.g. WT, PV) to provide some room for the harmonic and reactive power compensation. The maximum capacity of CCM DG units is also assumed to be 1500 W, and accordingly the rated apparent capacity of their inverters is set at 1650 VA. The maximum apparent capacity of VCM inverter is assumed to be 2500 VA.

### A. Simulation Study

Fig. 4 shows an MG which is considered in the simulation case study. This MG consists of two CCM units and one VCM unit which supply nonlinear and linear loads. The parameters of power and control systems are listed in Tables I and II, respectively. As shown in Table I, the line impedance of $DG_3$ is chosen to be two times of that of $DG_2$ for evaluating the performance of the control system with different line impedances.

The VCM unit operates from the beginning and then, the simulation is performed in the following steps:

- Step 1 (1s≤$t$<5s): Connecting CCM units ($DG_2$ and $DG_3$)
- Step 2 (5s≤$t$<8s): Activation of virtual impedance of DG1 as VCM unit
- Step 3 (8s≤$t$<11s): Activation of the proposed virtual admittance of CCM units
- Step 4 (11s≤$t$<15s): Activation of reactive reverse droop without considering distorted power for CCM units

This article has been accepted for publication in a future issue of this journal, but has not been fully edited. Content may change prior to final publication. Citation information: DOI 10.1109/TPEL.2018.2792780, IEEE Transactions on Power Electronics



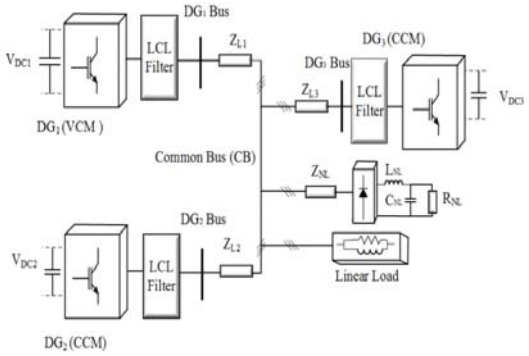


Fig. 4. Schematic of the case study system

TABLE I
Power Stage Parameters

| DC link voltage | | | LCL filter ($L_1$/C/$L_2$) | Voltage/ Frequency |
|---|---|---|---|---|
| 650V | | | For all DGs: 8.6mH/4.5μF/1.8mH | 230V/50Hz |
| Nonlinear Load | | | Linear load (simulation) | Linear load (experimental) |
| $C_{NL}$(μF) | $R_{NL}$(Ω) | $L_{NL}$(mH) | $Z_L$(Ω) | $Z_L$(Ω) |
| 235 | 114 | 0.084 | 95+82j | 200j |
| Line impedance | | | | |
| $Z_{L1}$(Ω) | | $Z_{L2}$(Ω) | $Z_{L3}$(Ω) | $Z_{NL}$ (Ω) |
| 0.1+0.5j | | 0.1+0.5j | 0.2+j | 0.1+0.5j |

TABLE II
Control Parameters

| Virtual admittance controller | | | | | | | |
|---|---|---|---|---|---|---|---|
| Allowable individual harmonic (%) | | | P controllers | | | Maximum admittance parameters | |
| $H_5^*$ | $H_7^*$ | $H_{11}^*$ | $K_{PH,5}$ | $K_{PH,7}$ | $K_{PH,11}$ | $K_{G7,5}$ | $K_{G11,5}$ |
| 1% | 1% | 0.5% | 100 | 100 | 100 | 1 | 1 |
| Maximum voltage deviation (ΔE) | | | Active power droop | | | | |
| 22 V | | | 0.00025 | | | | |
| Selective capacitive Virtual impedance for VCM | | | | | | | |
| $Z_{V1}$ | | $Z_{V5}$ | | $Z_{V7}$ | | $Z_{V11}$ | |
| j.ω. $1\times10^{-3}$ | | -j.5.ω. $L_2$ | | -j.7.ω. $L_2$ | | -j.11.ω. $L_2$ | |

- Step 5 (15s≤$t$<19s): Activation of the proposed reactive power droop and reverse droop controls, by taking into account distorted power ($S_N$)
- Step 6 (19s≤$t$≤22s): changing the reference of $DG_2$
- Step 7 (23s≤$t$≤26s): Increasing the linear load by 50%
- Step 8 (26s≤$t$≤29s): Decreasing the linear load to 50% of Step 6

Fig. 5(a) shows the harmonic content of output voltage of $DG_2$ ($V_{O2}$) while the harmonic content of $DG_3$ output voltage ($V_{O3}$) is similar to it. As mentioned in Section III.B, $V_{O2}$ and $V_{O3}$ are used as the input of virtual admittance and the 5th, 7th and 11th individual harmonics indexes ($H_5$, $H_7$ and $H_{11}$) of the voltage are regulated directly; As depicted in this figure, after activation of virtual admittance at Step 3, these indexes can track their reference values ($H_5^*$, $H_7^*$ and $H_{11}^*$) which are listed in Table 2 with small error. The small error occurs as a result of using P controller rather than PI controller in virtual admittance block as depicted in Fig. 3(a), since in islanded operation of MG, incorporation of the integrated term can endanger the harmonics sharing and stability when more than

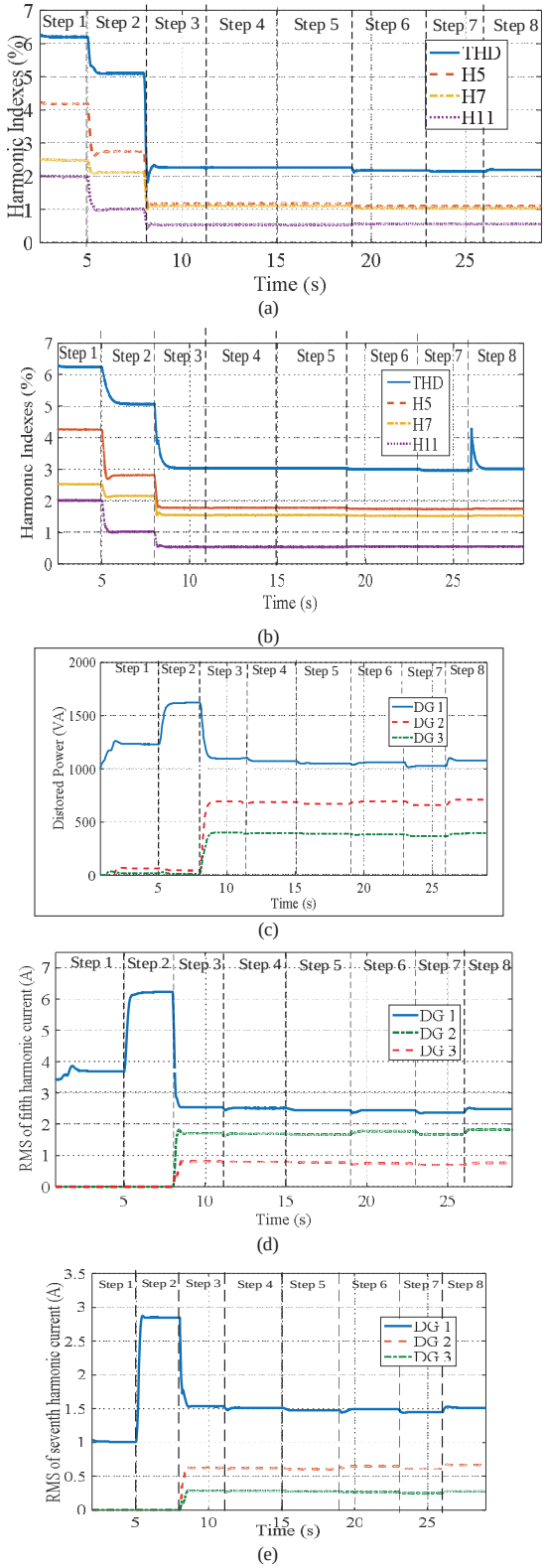


Fig. 5. Harmonics compensation analysis; (a) Harmonic contents of $V_{O2}$, (b) Harmonic contents of CB voltage, (c) Distorted power of DGs, (d) RMS value of 5th harmonic of DGs output currents ($i_2$), (e) RMS value of 7th harmonic of DGs output currents ($i_2$)

This article has been accepted for publication in a future issue of this journal, but has not been fully edited. Content may change prior to final publication. Citation information: DOI 10.1109/TPEL.2018.2792780, IEEE Transactions on Power Electronics



one CCM units contribute to harmonics compensation.

The 5th, 7th and 11th individual harmonics indices ($H_5$, $H_7$ and $H_{11}$) and total harmonic distortion (THD) of the CB voltage are depicted in Fig. 5(b). As can be seen in Figs. 5(a) and 5(b), the amount of all harmonics indices are decreased after the activation of virtual impedance of VCM unit at $t$=5s. As mentioned earlier, the compensation is achieved by using the capacitive virtual impedance of $DG_1$ which can mitigate the effect of output inductance of LCL filter ($L_2$). Furthermore, the figure shows that after the virtual admittance (conductance) activation of CCM units in Step 3, the harmonics compensation of the CB voltage is enhanced. In this mode, the CCM inverters act as active filters by creating a low impedance path for harmonic currents. Comparison of Figs. 5(a) and 5(b) shows that the harmonic indexes of CB voltage are higher than their related indexes of DGs output voltages which are regulated directly because of line impedances and using the DGs output voltages ($V_{O2}$ and $V_{O3}$) as local measurements.

Fig. 5(c) shows the distorted harmonic power ($S_N$) of DGs. It can be observed that after the activation of virtual impedance of $DG_1$ at Step 2, the $DG_1$ distorted power is increased and after the activation of virtual admittance of CCM units ($DG_2$ and $DG_3$) in Step 3, these DGs contribute to the compensation of harmonics. It can be seen in this figure that $DG_2$, which is electrically close to the nonlinear load ($Z_{L2}$<$Z_{L3}$), injects a larger harmonic current than $DG_3$. It is a desired situation since the power transmission losses are decreased in this case [24]. It is also shown that the entire remaining capacity of $DG_2$ is dedicated to the distorted power (i.e. $S_N = \sqrt{1650^2 - 1500^2} = 680$) in Step 5.

Fig. 5(d) also shows the RMS amounts of 5th order harmonics of DGs output currents ($i_2$ in Figs. 2 (a) and 2(b)), in order to depict the sharing of 5th harmonic currents. The RMS value is demonstrated here because $H_5$ depends on the fundamental component of current, and this component is changed in different steps for the evaluation of reactive power compensation. As depicted in this figure, after the virtual impedance activation in Step 2, the amount of 5th order harmonics current of $DG_1$ is increased, since the effect of the LCL filter output inductor ($L_2$) is compensated by inserting a virtual capacitance in 5th harmonics of $DG_1$. Furthermore, it shows that after the virtual admittance activation of CCM units, the 5th harmonic order components of $DG_2$ and $DG_3$ (as CCM units) currents are increased in Step 3, since they start harmonics compensation in this step. It can also be seen in this figure that 5th order harmonic of current of $DG_2$ is higher than 5th order harmonic current of $DG_3$ since $DG_2$ is closer to CB than $DG_3$. Fig. 5(e) shows the 7th harmonic current of DGs output current.

Figs. 6(a) and 6(b) show the CB voltage before and after compensation, respectively. This figure demonstrates a noticeable improvement in the voltage quality. This fact can also be confirmed by comparing the CB voltage THD in Steps 1 and 6 of Fig. 7(a).

Fig. 7(a) shows the delivered active powers by DG units. As shown in this figure, the CCM units can inject their reference powers (1500 W) to the MG in spite of harmonic distortion. In other words, injecting harmonics and reactive currents by the CCM units do not interfere with the active power injection.

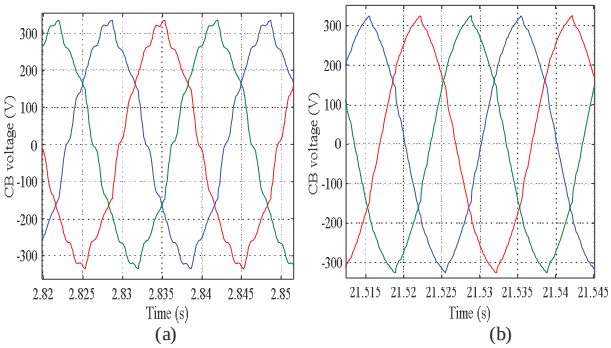


Fig. 7. Voltage waveform in simulation, (a) CB voltage waveform before compensation (Step 1), (b) CB voltage waveform after compensation (Step 6)

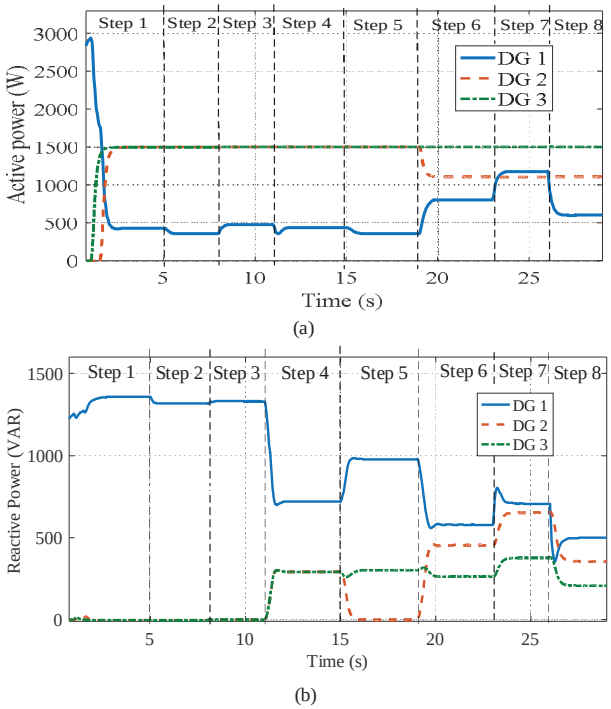


Fig. 7. Simulation results in different steps, (a) Active power, (b) Reactive power

Furthermore, the result shows that the step changing of DG2 reference power at $t$=19s does not affect the stability of the system. This figure also shows that by increasing the linear load in Step 7, the active powers delivered by DG1 (as VCM units) is increased while this powers is decreased in Step 8, since this unit regulates the frequency of the system by droop control without knowing about the load. It is assumed that the CCM reference powers are calculated by different systems such as master slave control, hierarchical control or coordinated control of CCM and VCM units [12] and calculation of it is not the scope of paper.

The reactive powers of the DG units are depicted in Fig. 7(b). As shown in this figure, the CCM inverters can contribute to the reactive power compensation after the activation of their reverse droop controls in Step 4 based on measurement of the DGs output voltages ($V_{O2}$ and $V_{O3}$). Before that, all of the reactive power of the load is provided by $DG_1$ which is

This article has been accepted for publication in a future issue of this journal, but has not been fully edited. Content may change prior to final publication. Citation information: DOI 10.1109/TPEL.2018.2792780, IEEE Transactions on Power Electronics



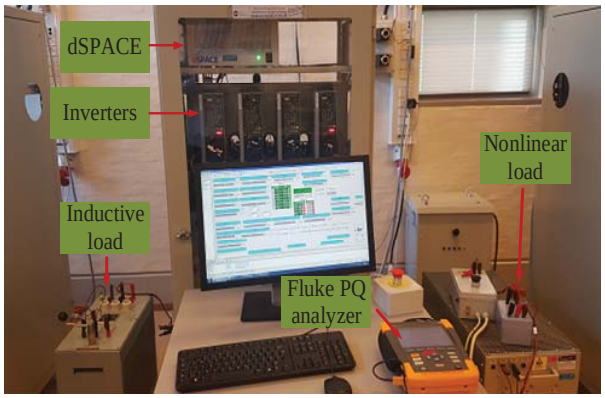


Fig. 8 Experimental setup scheme

working as VCM unit. The VCM unit regulates the voltage amplitude based on the droop control which is based on local measurement according to (1). It should be mentioned that for applying the proposed droop and reverse droop coefficients based on (7), the amount of $\Delta E$ is assumed to be 22 V which is lower than the 10% of rated voltage amplitude (230 V, phase RMS corresponding to 325 V phase amplitude) according to EN 50160 standard. After the activation of the proposed droop and reverse droop control and considering $S_N$ in Step 5, the reactive power of $DG_2$ is decreased to zero since its remaining capacity is dedicated to the harmonic compensation and SN provision (see Fig. 5(c)). It means that the slope of reverse droop which has been shown in Fig. 1(c) reaches zero for this DG according to (8). It can also be seen that considering the distorted power, $DG_2$ is prevented from overloading.

After decreasing the reference power of $DG_2$, the DG can contribute to reactive power support because the remaining capacity of the inverter is increased.

The figure also shows that by increasing the reactive power demanded by load in Step 7, the contribution of DGs is increased in order to regulate the voltage since increasing the reactive power demanded in load can cause a reduction in voltage due to the impedances voltage drop, and according to (2), the CCM units should inject more reactive power in order to restore the voltage. It is also shown in this figure that this contribution is decreased in Step 8, when the linear load is decreased.

### B. *Experimental Results*

For validation of the harmonic compensation and reactive power sharing, two DG units (one VCM and one CCM) are used in the experimental study by using a test system similar to Fig. 6, but, by having only $DG_1$ and $DG_2$. The parameters of the experimental setup are the same as the simulation study.

Fig. 8 shows the test bed, which consists of nonlinear and inductive loads, three-phase inverters, and dSPACE 1006 platform. A Fluke 437-II power quality analyzer is used for measuring the harmonic content of the CB voltage.

In the experimental study, the effectiveness of the harmonic compensation is investigated (initially without any reactive power support) first. At the beginning, the CCM and VCM units supply nonlinear and inductive loads without compensation. Afterward, the virtual impedance of VCM unit and the virtual admittance of CCM unit are enabled. Fig. 9

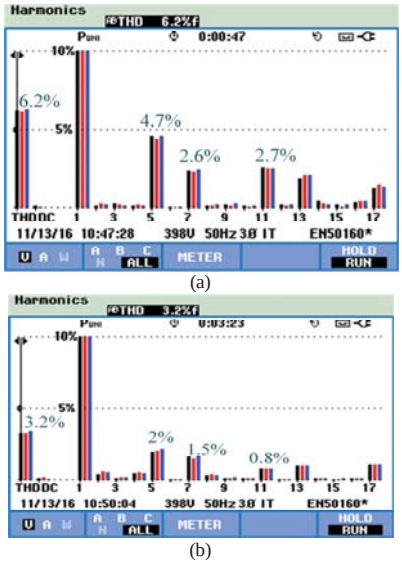


Fig. 9. Power quality report of power quality analyzer; (a) Before compensation; (b) After compensation

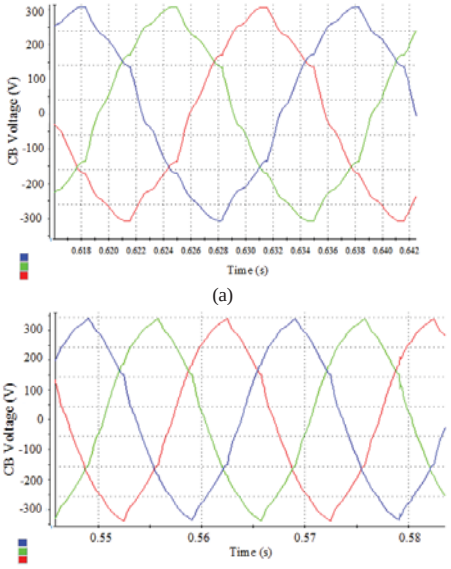


Fig. 10. Voltage in experimental study; (a) CB voltage before compensation, (b) After compensation

shows the harmonic content of measured CB voltage while its fundamental phase-voltage is 222 V. As shown in this figure, the THD of CB voltage is decreased from 6.2% to 3.2% due to compensation of the main individual harmonics ($5^{th}$, $7^{th}$ and $11^{th}$). This harmonic level is acceptable according to EN 50160 and IEEE 519 standards. Fig. 10 shows the CB voltage waveform before and after compensation.

As explained before, in the virtual impedance approach, the harmonic voltage drop of LCL filter is compensated by applying a voltage in the opposite phase of the distorting voltage drop; applying a voltage in the opposite phase of the distorting voltage drop; hence, the capacitor voltage will be distorted after activation of impedance in order to compensate the voltage drop of grid side inductance of LCL filter ($L_2$). The

This article has been accepted for publication in a future issue of this journal, but has not been fully edited. Content may change prior to final publication. Citation information: DOI 10.1109/TPEL.2018.2792780, IEEE Transactions on Power Electronics



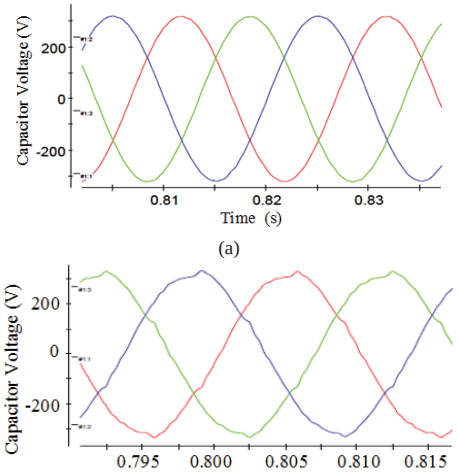


Fig.11 Capacitor voltage of VCM unit, (a) before virtual impedance activation, (b) after virtual impedance activation

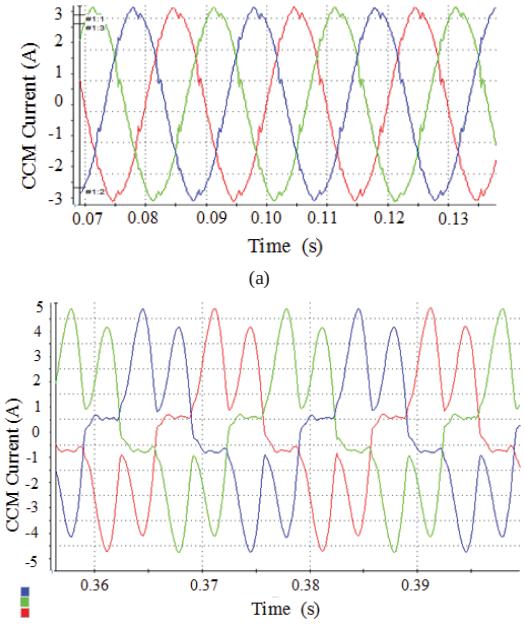


Fig.12 Output current of CCM unit, (a) before virtual admittance activation, (b) after virtual admittance activation

capacitor voltage of VCM units before and after virtual impedance activation is depicted in Figs. 11(a) and 11(b), respectively.

On the other hand, using the virtual admittance, a low impedance path for harmonic current is provided by the CCM unit. Figs. 12(a) and 12(b) show the CCM unit current before and after activation of virtual admittance. These figures verify the effectiveness of active damping method since no resonance can be observed in the current waveforms.

To evaluate the effectiveness of the proposed method from the reactive power sharing point of view, it is assumed that both VCM and CCM units are contributing in harmonics

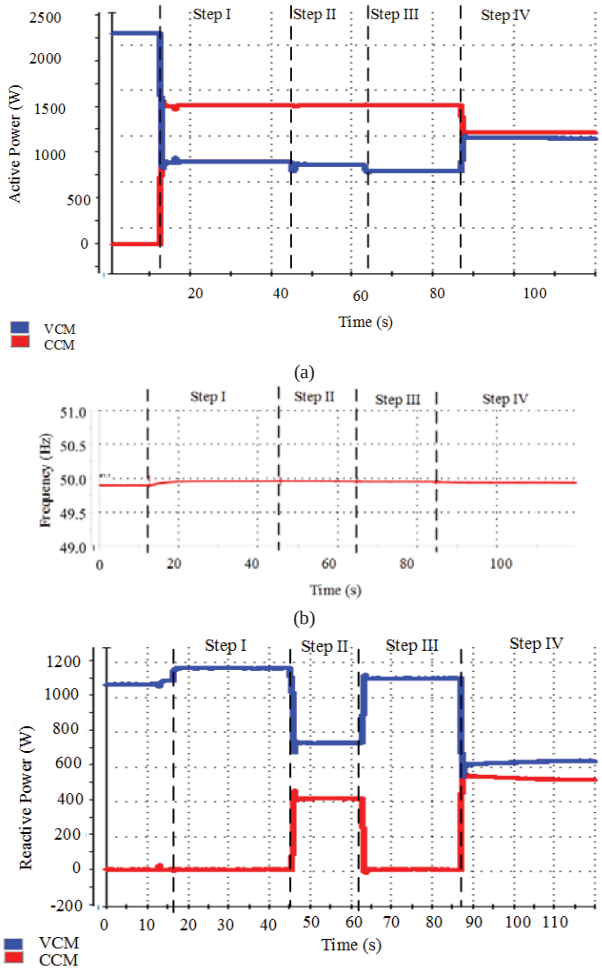


Fig. 13. Active and reactive powers and frequency in experimental; (a) Active power; (b) Frequency, (c) Reactive power

(virtual impedance and admittance of VCM and CCM units are activated) and afterward, the following four steps are taken:

- Step I: Connection of CCM unit without reactive power injection
- Step II: Activation of the reverse droop without considering distorted power
- Step III: Considering distorted power Step IV: Changing the reference power from 1500 W to 1200 W

Fig. 13(a) shows the active powers which are delivered by the DG units. As shown in this figure, the control system of CCM unit can track the reference active power in different steps. As depicted in this figure, since the frequency regulation is achieved by the droop control of VCM unit, the active power of the $DG_1$ (as VCM unit) is decreased after the connection of $DG_2$ while the active power of the $DG_1$ is increased when the reference power of the $DG_2$ is decreased. In other word, the VCM unit ($DG_1$) is responsible for providing the difference between the demanded active power and the active power derived by CCM unit ($DG_2$). The frequency of the microgrid

This article has been accepted for publication in a future issue of this journal, but has not been fully edited. Content may change prior to final publication. Citation information: DOI 10.1109/TPEL.2018.2792780, IEEE Transactions on Power Electronics



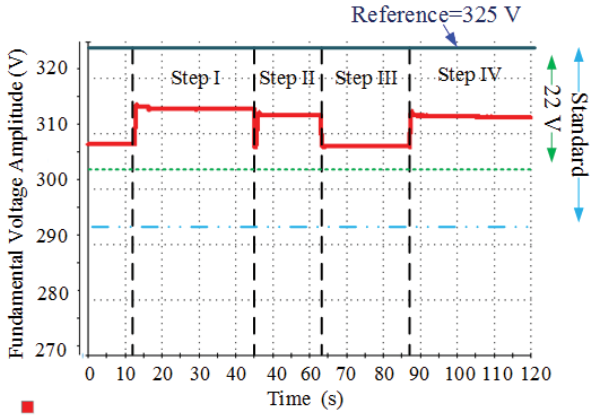


Fig. 14. CB Voltage amplitude in experimental study

is shown in Fig. 13 (b). Fig. 13(c) shows the reactive power of DG units. As depicted in this figure, after the activation of reverse droop control in Step II, the CCM unit can contribute to the reactive power support. By considering the distorted power (Step III), the available reactive powers of CCM and VCM units are decreased. The result shows that the CCM unit cannot inject reactive power since all of the capacity is dedicated to active and distorted powers in Step III.

In Step IV, more remaining capacity is available due to the decrease in the reference active power of CCM unit; thus, the CCM unit contributes more to the reactive power support.

The amplitude of fundamental component of the CB voltage is depicted in Fig. 14. As shown in this figure, in all steps, the voltage amplitude is well above the value associated with the maximum 22V drop which is considered for the proposed reactive power sharing method and also specified by standard limit of EN 50160.

## V. Conclusion

In this paper, a decentralized harmonic compensation and reactive power coordination method is proposed for VCM and CCM units in an islanded MG. The harmonic compensation is achieved by using virtual capacitive impedance and conductive admittance for VCM and CCM units, respectively. The proposed virtual admittance is adaptively changed in different values of reference power of CCM units according to the available capacity of the inverter. Furthermore, modified reactive droop and reverse droop control schemes are proposed for VCM and CCM units, respectively to take their available capacity into account. This coordinated control of CCM and VCM units are implemented using only local measurement; hence, the communication systems and central controllers are not required.

Simulation and experimental results show that by applying virtual admittance and impedance approaches the CB voltage harmonics compensation is achieved properly. Furthermore, the CCM and VCM units can contribute to reactive power compensation depending on their remaining capacity using the proposed reactive power compensation approach. Thus, this scheme is effective in applications such as photovoltaic systems where the active power generation is changing throughout the day.

## References

[1] T.C. Green and M. Prodanović, "Control of inverter-based micro grids," Electric Power Systems Research, vol. 77, pp. 1204–1213, 2007.

[2] F. Blaabjerg, Z. Chen; S. B Kjaer, "Power electronics as efficient interface in dispersed power generation systems," IEEE Trans. Power Electron., vol. 19, no. 5, pp. 1184-1194, Sept. 2004.

[3] J. Rocabert, A. Luna, F. Blaabjerg, P. Rodriguez, "Control of power converters in AC microgrids," IEEE Trans. Power Electron., vol. 27, no. 11, pp. 4734-4749, Nov. 2012.

[4] D. Wu, F. Tang, T. Dragicevic, J. C. Vasquez and J. M. Guerrero, "A control architecture to coordinate renewable energy sources and energy storage systems in islanded Microgrids," IEEE Trans. Smart Grid, vol. 6, no. 3, pp. 1156-1166, May 2015.

[5] I. Serban, C. Marinescu, "Control strategy of three-phase battery energy storage systems for frequency support in microgrids and with uninterrupted supply of local loads,", IEEE Trans. Power Electron., vol. 29, no. 9, pp. 5010-5020, Sept. 2014.

[6] J.M Guerrero, M. Chandorkar, T. Lee, P.C. Loh, "Advanced control architectures for intelligent microgrids—part I: decentralized and hierarchical control," IEEE Trans. Ind. Electron., vol. 60, no. 4, pp. 1254-1262, April 2013.

[7] Q. Shafiee, J. M. Guerrero and Juan C. Vasquez, " Distributed secondary control for islanded microgrids - a novel approach", IEEE Trans. Power Electron., vol. 29, pp. 1018 – 1031, Feb. 2014.

[8] A. Tuladhar, H. Jin, T. Unger, and K. Mauch, "Control of parallel inverters in distributed ac power systems with consideration of line impedance effect", IEEE Trans. Ind. Appl., vol. 36, no. 1, pp. 131-138, Jan./Feb. 2000.

[9] E. Demirok et al., "Local reactive power control methods for overvoltage prevention of distributed solar inverters in low-voltage grids," IEEE J. Photovolt., vol. 1, no. 2, pp. 174–182, Oct. 2011.

[10] E. Ghiani, and F. Pilo, "Smart inverter operation in distribution networks with high penetration of photovoltaic systems," J. Mod. Power Syst. Clean Energy, vol. 3, no. 4, pp. 504–511, Dec. 2015.

[11] Dan Wu, F. Tang, J.M Guerrero, J.C Vasquez, G. Chen and L. Sun, "Autonomous active and reactive power distribution strategy in islanded microgrids," Twenty-Ninth Annual IEEE Applied Power Electron. Conf. and Exposition (APEC), pp. 2126-2131, March 2014.

[12] Dan Wu, Fen Tang, J. C. Vasquez and J. M. Guerrero, "Control and analysis of droop and reverse droop controllers for distributed generations," 11th International Multi-Conf. on Systems, Signals & Devices (SSD) , pp. 1-5,Barcelona, 2014.

[13] H. Akagi, "New trends in active power filters for power conditioning," IEEE Trans. Ind. Appl., vol. 32, no. 6, pp. 1312-1322, Nov/Dec.1996.

[14] Zh. Zeng, H. Yang, R. Zhao, Ch. Cheng, Zh. Zeng, H. Yang, R. Zhao and Ch. Cheng, "Topologies and control strategies of multi-functional grid-connected inverters for power quality enhancement: A comprehensive review" Renewable and Sustainable Energy Reviews, vol. 24, pp. 223–270, Aug. 2013.

[15] Savaghebi, M.; Jalilian, A.; Vasquez, J.C.; Guerrero, J.M., "Secondary control for voltage quality enhancement in microgrids," IEEE Trans Smart Grid, vol. 3, no. 4, pp. 1893-1902, Dec. 2012.

[16] M. Savaghebi, Q. Shafiee, J. C. Vasquez and J. M. Guerrero, "Adaptive virtual impedance scheme for selective compensation of voltage unbalance and harmonics in microgrids," IEEE Power & Energy Society General Meeting, Denver, CO, pp. 1-5, 2015.

[17] X. Wang, F. Blaabjerg, and Z. Chen, "Synthesis of variable harmonic impedance in inverter-interfaced distributed generation unit for harmonic resonance damping throughout a distribution network," IEEE Trans. Ind. Appl., vol. 48, no. 4, pp. 1407-1417, Jul./Aug. 2012.

[18] Xiongfei Wang; Blaabjerg, F.; Zhe Chen, "Autonomous control of inverter-interfaced distributed generation units for harmonic current filtering and resonance damping in an islanded microgrid," IEEE Trans. Ind. Appl., vol. 50, no. 1, pp. 452-461, Jan.-Feb. 2014.

[19] A. Micallef; M. Apap; C. Spiteri-Staines; J. M. Guerrero, "Mitigation of harmonics in grid-connected and islanded microgrids via virtual admittances and impedances," IEEE Trans. Smart Grid, vol. 8, no.2, pp. 651-661, 2017

[20] Jinwei He; Yun Wei Li; F. Blaabjerg, “flexible microgrid power quality enhancement using adaptive hybrid voltage and current controller,” IEEE Trans. Ind. Electron., vol. 61, no. 6, pp. 2784-2794, June 2014.
[21] J. He, B. Liang, Y. W. Li and C. Wang, "Simultaneous microgrid voltage and current Harmonics compensation using coordinated control of dual-interfacing converters," IEEE Trans. Power Electron., vol. 32, no. 4, pp. 2647-2660, April 2017.
[22] Z. Zeng, H. Yang, S. Tang and R. Zhao, “Objective-oriented power quality compensation of multifunctional grid-tied inverters and its application in microgrids,” IEEE Trans. Power Electron., vol. 30, no. 3, pp. 1255-1265, March 2015.
[23] Zheng Zeng; Rongxiang Zhao; Huan Yang, “Coordinated control of multi-functional grid-tied inverters using conductance and susceptance limitation,” IET Power Electron., vol. 7, no. 7, pp. 1821- 1831, July 2014.
[24] C. Blanco, D. Reigosa, J. C. Vasquez, J. M. Guerrero and F. Briz, “Virtual admittance loop for voltage harmonic compensation in microgrids,” IEEE Trans. Ind. Appl., vol. 52, no. 4, pp. 3348-3356, July-Aug. 2016.
[25] IEEE Standard Definitions for the Measurement of Electric Power Quantities Under Sinusoidal, Nonsinusoidal, Balanced, or Unbalanced Conditions," IEEE Std 1459-2010 (Revision of IEEE Std 1459-2000) , pp. 1-50, March 2010.
[26] D. Wu, F. Tang, T. Dragicevic, J. C. Vasquez and J. M. Guerrero, “Autonomous active power control for islanded AC microgrids with photovoltaic generation and energy storage system,” IEEE Trans. Energy Conv., vol. 29, no. 4, pp. 882-892, Dec. 2014.
[27] M. Chandorkar, D. Divan, and R. Adapa, “Control of parallel connected inverters in standalone AC supply systems,” IEEE Trans. Ind. Appl.,vol. 29, no. 1, pp. 136–143, Jan./Feb. 1993.
[28] Y. Li, D.M. Vilathgamuwa, P.C. Loh “Design, analysis, and real-time testing of a controller for multi-bus microgrid system” IEEE Trans. Power Electron., vol. 19 no. 5 pp. 1195–1204, Sept. 2004.
[29] A. Luna; L. Meng; N. Diaz Aldana; M. Graells; J. Vasquez; J. Guerrero, "Online energy management systems for microgrids: experimental validation and asessment framework," IEEE Trans. Power Electron. , Early Access, 2017.
[30] G. Oriti, A. L. Julian, and N. J. Peck, “Power-electronics-based energy management system with storage,” IEEE Trans. Power Electron., vol. 31, no. 1, pp. 452–460, Jan 2016.
[31] C. Gouveia, J. Moreira, C. L. Moreira and J. A. Peças Lopes, "Coordinating storage and demand response for microgrid emergency operation," IEEE Trans. Smart Grid, vol. 4, no. 4, pp. 1898-1908, Dec. 2013.
[32] H. Akagi, Yoshihira Kanazawa and A Nabae, “Instantaneous reactive power compensators comprising switching devices without energy storage components,” IEEE Trans. Industry Appl., vol. IA-20, no.3, pp.625-630, May 1984.
[33] J. C. Vasquez, J. M. Guerrero, M. Savaghebi, J. Eloy-Garcia and R. Teodorescu, “Modeling, analysis, and design of stationary-reference-frame droop-controlled parallel three-phase voltage source inverters,” IEEE Trans. Ind. Electron, vol. 60, no. 4, pp. 1271-1280, April 2013.
[34] P. Rodriguez, A. Luna, I. Candela, R. Mujal, R. Teodorescu and F. Blaabjerg, “Multiresonant frequency-locked loop for grid synchronization of power converters under distorted grid conditions,” IEEE Trans. Ind. Electron., vol. 58, no. 1, pp. 127-138, Jan. 2011.
[35] M. Liserre, R. Teodorescu, and F. Blaabjerg, “Stability of photovoltaic and wind turbine grid-connected inverters for a large set of grid impedance values,” IEEE Trans. Power Electron., vol. 21, no. 1, pp. 263–272, Jan. 2006.
[36] Poh Chiang Loh and D. G. Holmes, “Analysis of multiloop control strategies for LC/CL/LCL-filtered voltage-source and current-source inverters,” IEEE Trans Ind. Appl., vol. 41, no. 2, pp. 644-654, March-April 2005.
[37] Ch. Bao, X. Ruan, X. Wang, W. Li, D. Pan, and K.Weng. “Step-by-Step Controller Design for LCL-Type Grid-Connected Inverter with Capacitor–Current-Feedback Active-Damping” IEEE Trans. Power Electron., vol. 29, no. 3, March 2014.
[38] J. Xu, S. Xie and T. Tang, "Active damping-based control for grid-connected LCL -filtered inverter with injected grid current feedback only," IEEE Trans. Ind. Electron. vol. 61, no. 9, pp. 4746-4758, Sept. 2014.
[39] EN 50160 standard, “Voltage characteristics of electricity supplied by public distribution systems,” 1999.
[40] IEEE 519 Standard "IEEE Recommended Practice and Requirements for Harmonic Control in Electric Power Systems", 2014.

Seyyed Yousef Mousazadeh Mousavi was born in Babol, Iran, in 1987. He received the B.Sc. degree from Mazandaran University (Babol University of Technology), Iran, with highest honors in 2010 and the M.Sc. degree from Amirkabir University of technology in 2012 all in Electrical Engineering. Currently, he is Ph.D. student at Iran University of Science and Technology. From 2013 to 2014, he was a Lecturer in this University.
In 2016, he was a visiting Ph.D. Student with the Department of Energy Technology, Aalborg University, Aalborg, Denmark. His main research interests include power electronics, distributed generation systems, microgrids and power quality.

**Alireza Jalilian** was born in Yazd, Iran, in 1961. He received the B.Sc. degree in electrical engineering from Mazandaran University, Babol, Iran, in 1989, and the M.Sc. and Ph.D. degrees from University of Wollongong, Wollongong, NSW, Australia, in 1992 and 1997, respectively. He joined the power group of the school of electrical engineering at Iran University of Science and Technology in 1998, where he is an Associate Professor. Dr Jalilian is a member of Centre of Excellence for Power System Automation and Operation at IUST. He is also head of Power Quality Laboratory at IUST where he has supervised more than 100 Ph.D., M.SC. and B.Sc. research students in different projects mostly in the area of Electric Power Quality. His research interests are causes, effects and mitigation of power quality problems in electrical systems and microgrids. Since 1997, Dr Jalilian, has been a reviewer for several IEEE Transactions, IET and Elsevier journals and a member of technical committee of several national and international conferences. In 2006, Dr Jalilian joined the department of electrical engineering, University of West of England, Bristol, UK as visiting professor for his sabbatical. He was also a visiting professor at the department of electrical engineering, University of British Columbia (UBC) for six months in 2017.

Mehdi Savaghebi (S’06-M’15-SM’15) was born in Karaj, Iran, in 1983. He received the B.Sc. degree from University of Tehran, Iran, in 2004 and the M.Sc. and Ph.D. degrees with highest honors from Iran University of Science and Technology, Tehran, Iran in 2006 and 2012, respectively, all in Electrical Engineering. From 2007 to 2014, he was a Lecturer in Electrical Engineering Department, Karaj Branch, Islamic Azad University where he taught various courses and conducted research on power systems and electrical machines. In 2010, he was a visiting Ph.D. Student with the Department of Energy Technology, Aalborg University, Aalborg, Denmark and with the Department of Automatic Control Systems and Computer Engineering, Technical University of Catalonia, Barcelona, Spain.
Currently, he is an Associate Professor in the Department of Energy Technology, Aalborg University. His main research interests include distributed generation systems, microgrids, power quality, Internet of Things (IoT) and smart metering. Dr. Savaghebi has been a Guest Editor of Special Issue on Power Quality in Smart Grids, IEEE Transactions on Smart Grid. He is a member of Technical Committee of Renewable Energy Systems, IEEE Industrial Electronics Society and also IEEE Task Force on Microgrids Stability Analysis and Modeling.

**Josep M. Guerrero** (S'01-M'04-SM'08-FM'15) received the B.S. degree in telecommunications engineering, the M.S. degree in electronics engineering, and the Ph.D. degree in power electronics from the Technical University of Catalonia, Barcelona, in 1997, 2000 and 2003, respectively. Since 2011, he has been a Full Professor with the Department of Energy Technology, Aalborg University, Denmark, where he is responsible for the Microgrid Research Program (www.microgrids.et.aau.dk). From 2012 he is a guest Professor at the Chinese Academy of Science and the Nanjing University of Aeronautics and Astronautics; from 2014 he is chair Professor in Shandong University; from 2015 he is a distinguished guest Professor in Hunan University; and from 2016 he is a visiting professor fellow at Aston University, UK, and a guest Professor at the Nanjing University of Posts and Telecommunications.

His research interests is oriented to different microgrid aspects, including power electronics, distributed energy-storage systems, hierarchical and cooperative control, energy management systems, smart metering and the internet of things for AC/DC microgrid clusters and islanded minigrids; recently specially focused on maritime microgrids for electrical ships, vessels, ferries and seaports. Prof. Guerrero is an Associate Editor for the IEEE TRANSACTIONS ON POWER ELECTRONICS, the IEEE TRANSACTIONS ON INDUSTRIAL ELECTRONICS, and the IEEE Industrial Electronics Magazine, and an Editor for the IEEE TRANSACTIONS on SMART GRID and IEEE TRANSACTIONS on ENERGY CONVERSION. He has been Guest Editor of the IEEE TRANSACTIONS ON POWER ELECTRONICS Special Issues: Power Electronics for Wind Energy Conversion and Power Electronics for Microgrids; the IEEE TRANSACTIONS ON INDUSTRIAL ELECTRONICS Special Sections: Uninterruptible Power Supplies systems, Renewable Energy Systems, Distributed Generation and Microgrids, and Industrial Applications and Implementation Issues of the Kalman Filter; the IEEE TRANSACTIONS on SMART GRID Special Issues: Smart DC Distribution Systems and Power Quality in Smart Grids; the IEEE TRANSACTIONS on ENERGY CONVERSION Special Issue on Energy Conversion in Next-generation Electric Ships. He was the chair of the Renewable Energy Systems Technical Committee of the IEEE Industrial Electronics Society. He received the best paper award of the IEEE Transactions on Energy Conversion for the period 2014-2015, and the best paper prize of IEEE-PES in 2015. As well, he received the best paper award of the Journal of Power Electronics in 2016. In 2014, 2015, and 2016 he was awarded by Thomson Reuters as Highly Cited Researcher, and in 2015 he was elevated as IEEE Fellow for his contributions on "distributed power systems and microgrids."